

# Urban Near-surface Seismic Monitoring using Distributed Acoustic Sensing

Gang Fang<sup>1,2</sup>, Yunyue Elita Li<sup>1</sup>, Yumin Zhao<sup>1</sup>, and Eileen R. Martin<sup>3</sup>

<sup>1</sup>Department of Civil and Environmental Engineering, National University of Singapore, Singapore

<sup>2</sup>Key Laboratory of Marine Hydrocarbon Resources and Environmental Geology, Ministry of Land and Resources, Qingdao Institute of Marine Geology, Qingdao, 266071, China

<sup>3</sup>Department of Mathematics, Program in Computational Modeling and Data Analytics, Virginia Tech, Virginia, USA

## Key Points:

- Using the Stanford DAS data, we demonstrate the reliability and sensitivity of surface deployed DAS in urban subsurface monitoring.
- Short DAS recordings of far-field quarry blasts show sensitivity to the changes in near-surface velocity within the footprint of the DAS array.
- DAS can play an important role in many applications of real time, high resolution, long term monitoring in urban environments.

---

Corresponding author: Yunyue Elita Li, [ceeliyy@nus.edu.sg](mailto:ceeliyy@nus.edu.sg)

## Abstract

Urban subsurface monitoring requires a system with high temporal-spatial resolution, low maintenance cost, and minimal intrusion to urban life. Distributed acoustic sensing (DAS), in contrast to conventional station-based sensing technology, has the potential to provide a passive seismic solution to urban monitoring requirements. Based on data recorded by the Stanford Fiber Optic Seismic Observatory, we demonstrate that near-surface velocity change induced by the excavation of basement construction can be monitored using existing fiber optic infrastructure in a noisy urban environment. To achieve the superior results, careful signal processing with noise removal and source signature normalization are applied to raw DAS recordings. The repeated blast signals from quarry sites provide free, unidirectional, and near impulsive sources for periodic urban seismic monitoring, which are essential for increasing the temporal resolution of passive seismic methods. Our study suggests that DAS will likely play an important role in urban subsurface monitoring.

## 1 Plain Language Summary

Seismic monitoring can provide crucial information about near-surface changes due to natural or manmade activities. However, the high cost and the "after-effect" nature of conventional station-based monitoring methods limit their application in urban environments where near real-time and meter-scale resolution are required. Distributed acoustic sensing (DAS) has the potential to achieve all requirements utilizing existing communication infrastructure. Using Stanford Fiber Optic Seismic Observatory, we demonstrate that its recordings of quarry blasts 13.3 *km* away carry important subsurface velocity information within the footprint of the array. These short bursts of quarry blast signals provide us free, unidirectional, and repetitive sources that sample the urban subsurface at an interval frequent enough for monitoring. We observe large velocity decrease from the recordings close to the excavation site. Our study suggests that telecommunications fiber repurposed for DAS will potentially play an important role in many urban subsurface monitoring applications.

## 2 Introduction

Characterizing and monitoring changes in the top tens of meters of the Earth's subsurface will play a significant role to satisfy the increasing need of urban sustainability and resilience (Díaz et al., 2017). Near-surface changes due to natural or man-made events may lead to hazards including ground subsidence (Tran & Sperry, 2018), sinkholes (Dahm et al., 2011; Gutiérrez et al., 2014), and landslides (Renalier et al., 2010; Schenato et al., 2017), which may result in direct casualties of urban residents and damages to existing infrastructure (Douglas, 2004). Many such subsurface changes manifest themselves as temporal variations in geophysical properties (such as velocity, attenuation, electric conductivity, gravity, etc.) before catastrophic hazards occur, which can be monitored and predicted by geophysical prospecting using seismic, electric, electromagnetic and gravitational methods.

Compared to conventional geophysical exploration for resources, near-surface monitoring in urban environments has the unique acquisition requirements of: 1) high spatial resolution towards meter-scale; 2) high temporal resolution towards real-time data collection and daily warning; 3) low maintenance for long term monitoring; and 4) minimal intrusion to urban life. These requirements are met by a densely distributed, frequently recording, easy to maintain, passive system that we present in this paper: a passive seismic monitoring system enabled by distributed acoustic sensing (DAS). A DAS array measures strain along kilometers of optical fiber, producing large datasets with kilohertz time sampling and at sub-meter channel spacing (Parker et al., 2014). Over the past dozen years, DAS has been a rapidly evolving technology for vertical seismic pro-

66 filing (VSP) in oil and gas reservoirs (Willis et al., 2016). Recent success of DAS appli-  
 67 cations using existing telecommunication infrastructures (Jousset et al., 2018; Yu, 2019;  
 68 Ajo-Franklin et al., 2019) demonstrates its cost-effectiveness in deployment and main-  
 69 tenance. However, these experiments are conducted in remote areas for applications in  
 70 earthquake and microseismic monitoring, where anthropogenic noise is rare and desired  
 71 signal is clearly visible above the random noise in DAS measurements.

72 DAS arrays deployed in urban environments are reported that near-surface veloci-  
 73 ties can be estimated with ambient noise recorded by DAS over month-long periods (Dou  
 74 et al., 2017; Martin et al., 2018; Spica et al., 2019, July 16). Long observation times are  
 75 needed to combat strong near-field anthropogenic noise, but severely limits the tempo-  
 76 ral resolution of passive seismic monitoring with DAS. Here we present a case study with  
 77 the Stanford Fiber Optic Seismic Observatory where we take advantage of far-field an-  
 78 thropogenic activities - quarry blasts - to monitor the near-field anthropogenic activity  
 79 - excavation. The weekly quarry blasts inspect the subsurface with sufficient energy at  
 80 intervals relevant to urban monitoring. We perform careful signal processing to reduce  
 81 the effect of strong near-field noise and the variability in the blast sources. We demon-  
 82 strate that with 100 seconds of DAS recordings after quarry blasts, near-surface veloc-  
 83 ity change caused by construction of a basement within the array is observed.

### 84 **3 Data and Signal Processing**

#### 85 **3.1 Stanford Fiber Optic Seismic Observatory data acquisition**

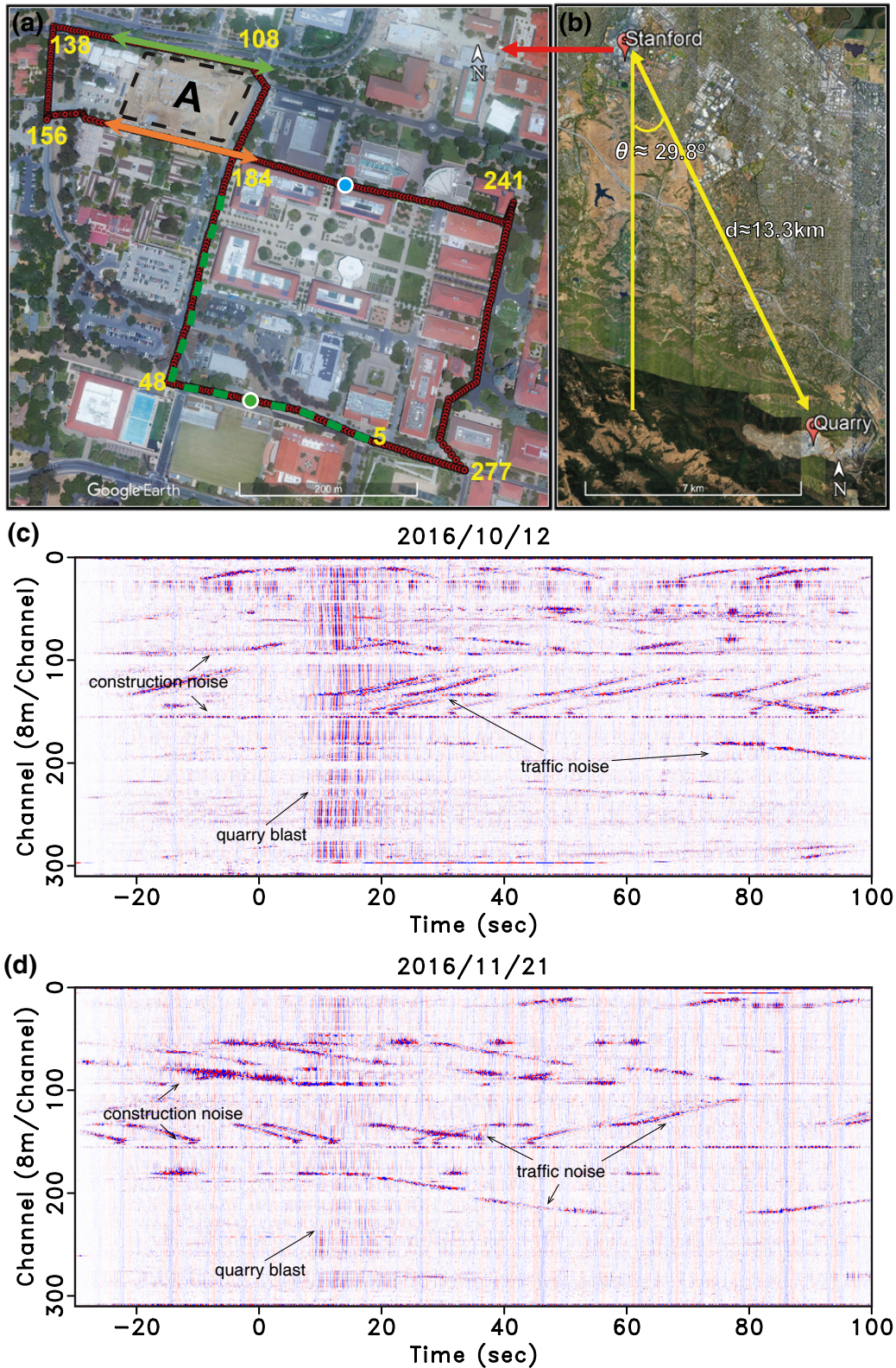
86 The Stanford Fiber Optic Seismic Observatory (also called Stanford DAS Array) (Biondi  
 87 et al., 2017) is one of the first DAS surface arrays to use existing telecommunications in-  
 88 frastructure, and is the longest-running ultra-dense urban seismic study in the world.  
 89 In this experiment, 2.5 kilometers of fiber-optic cable is deployed loosely in existing un-  
 90 derground telecommunication conduits (typically 10–15 cm wide PVC pipe) under the  
 91 Stanford University campus. Coupling between the fiber cable and the surrounding con-  
 92 duit relies only on gravity and friction. This experiment simulates DAS acquisition us-  
 93 ing dark fibers in the existing telecommunication system. Figure 1a shows the footprint  
 94 of the DAS array, which recorded data at a 25 Hz Nyquist frequency with 8.16 m chan-  
 95 nel spacing and 7.14 m gauge length. Construction of a basement (labeled with "A" in  
 96 Figure 1a) began its excavation on 7 November 2016.

#### 102 **3.2 Quarry blasts data**

103 Lehigh Permanente Quarry is located 13.3 km away 29.9° southeast of the DAS ar-  
 104 ray (Figure 1b). Figures 1c and 1d show the DAS recordings on 12 October 2016 18 :  
 105 30 : 16.9 UTC and on 21 November 18 : 56 : 12.5 UTC, after applying a bandpass fil-  
 106 ter from 0.25 to 2.5 Hz. The origin of the time axis denotes the blasting time provided  
 107 by the data recorded by a USGS seismometer at the "Jasper Ridge Biological Preserve"  
 108 that is managed by the Berkeley Digital Seismic Network. The near vertical events come  
 109 from the quarry blasts, whereas strong dipping events are the direct impact of traffic on  
 110 the fiber and the horizontal events are construction noise. We observe polarity flips around  
 111 the corner of each pair of orthogonal segments of the DAS array (Figures 1c and 1d and  
 112 Movie S1 in supporting information), which is caused by the angular sensitivity of DAS  
 113 strain measurements (Lindsey et al., 2017).

114 In the subsequent signal processing, we aim to extract subsurface information based  
 115 on far-field quarry blasts while minimizing the influence of near-field anthropogenic noise.  
 116 Figures 2a and 2b zoom in on two blast signals after geometric polarity correction (Biondi  
 117 et al., 2017). Because of the strong surface wave energy and anthropogenic noise (mainly  
 118 traffic and construction noise) during the daytime, it is hard to identify any body wave  
 119 from the profiles. Based on the fact that the quarry blasts events sweep through the DAS





97 **Figure 1.** (a) Layout of the DAS array with the corner points labeled by the corresponding  
 98 channel numbers. The green and blue dots are virtual sources used for seismic interferometry  
 99 in Figures 4 and 5, respectively. (b) Location of the quarry relative to the DAS array. (c) and  
 100 (d) Bandpassed DAS recordings on 12 October 2016 and 21 November 2016, respectively. Site A  
 101 boxed by the black dashed line denotes the basement construction site.

array in a non-perpendicular uniform direction, a combination of Rayleigh and Love waves are expected to be observed by DAS array. The blast vibration events reached to the south portion of the array (Channel 5) almost 0.7s earlier than they reached the north portion (channel 138). This time lag matches the relative distance and the average velocity between these two portions of the array, which is estimated in the next section. The blue lines overlaid on the profiles of Figures 2a and 2b are the single-channel response of channel 120. Figures 2c and 2d show their time-frequency spectrograms, respectively. Note that the main energy of the two quarry blasts events arrives at the DAS array around 14s after the explosion. Their dominant frequencies are approximately 1.2 Hz.

MUSIC beamforming (Zhang et al., 2019) is applied on the southwest corner of the DAS array (indicated by green dashed line in Figure 1a) within a small time window of 10-15s (labeled with the red dashed box in Figures 2a and 2b), which is selected in a relatively quiet zone and can help MUSIC beamforming obtain accurate results. Figures 2e, 2f and movie S2 in supporting information show the MUSIC spectrum results of different day's data. Their peaks roughly indicate the wavefield propagation direction and velocity, from which we conclude that the quarry blasts provide us an unidirectional source for this monitoring. Although the quarry blasts signals recorded at different times show certain similarity, their waveform are complex and quite different as shown by the blue lines in Figures 2a and 2b. The reason for this difference may lie in the randomness of explosive energy, excitation environment and the ragged earth surface where the source is excited. Compounding this issue, as the wavefield arrives at the DAS array, the waveform is scattered by strong velocity contrasts between Earth materials and underground infrastructures. Meanwhile, urban noise further contaminates the signals.

### 3.3 Signal processing

We propose a data processing workflow to reduce the impacts of urban noise and waveform differences. It starts with raw DAS records and results in cross-correlograms between virtual sources and other channels, which are used for velocity estimation. The workflow is the same for all quarry blasts, yet parameters are tuned on a daily basis.

**Bandpass, FK and median filter:** A Butterworth bandpass filter with cut-off frequencies from 0.25 Hz to 2.5 Hz is applied to all quarry blast data. A dip filter is applied to remove the high frequency but low dip coherent events in the frequency-wavenumber(FK) domain. Those noises are primarily generated by direct traffic impact or the equipment on construction sites. Therefore, the parameters to control the dip filter are tuned daily according to noise on that day. A sliding 2-D medians filter is used to remove spike noise for all the data.

**Normalized cross-correlation:** The quarry sets off each blasts with different source signature. We use normalized cross-correlation to eliminate the imprint of the source signature. Under the assumption of plane wave propagation, the signals recorded at receivers  $R_A$  and  $R_B$  in the frequency domain can be written as follows

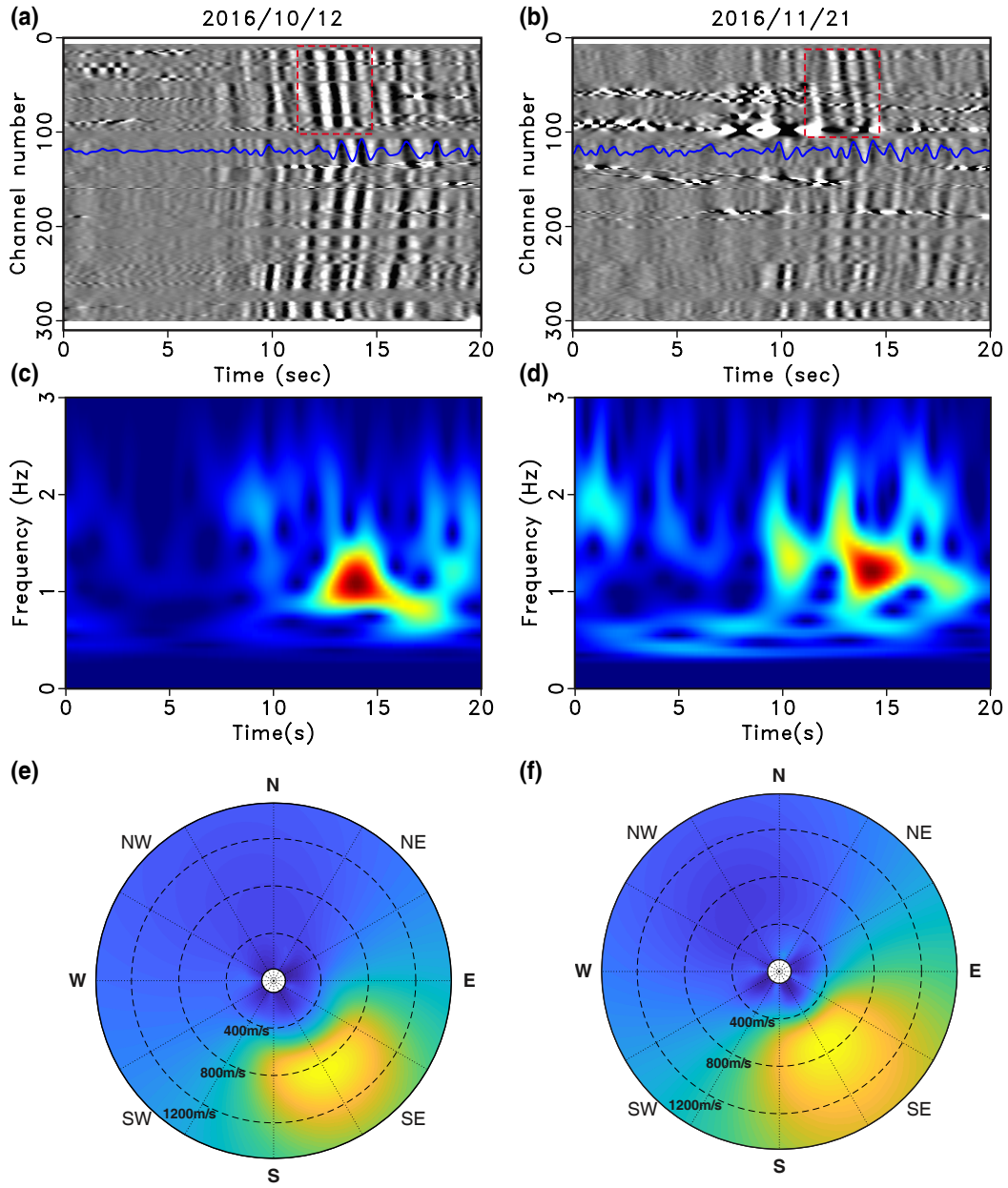
$$U(R_A, \omega) = S(R_S, \omega)e^{ik(R_A - R_S)}, \quad (1)$$

$$U(R_B, \omega) = S(R_S, \omega)e^{ik(R_B - R_S)}, \quad (2)$$

where  $S(R, \omega)$  is the source spectrum,  $k$  is the wavenumber. The normalized cross-correlation operator is defined as

$$C_N(R_A, R_B, \omega) = \frac{U(R_A, \omega)U^*(R_B, \omega)}{\langle\langle |U(R_A, \omega)||U^*(R_B, \omega)| \rangle\rangle} \approx e^{ik(R_A - R_B)}, \quad (3)$$

where  $\langle\langle \cdot \rangle\rangle$  is a Gaussian smoothing operator,  $|\cdot|$  denotes the absolute value operator. Equation 3 can both remove the influence of the source wavelet and improve the data resolution. More details of data processing results can be found in supporting information Figures S1-S2.



143 **Figure 2.** Quarry blasts DAS data on (a) 12 October 2016 and (b) 21 November 2016. Both  
 144 plots (a) and (b) are after noise attenuation and polarity flip correction. Blue lines denote the  
 145 signals of channel 120. Plots (c) and (d) compare the time frequency spectrograms of these two  
 146 days data, which is calculated with the single channel shown with blue lines in plot (a) and (b),  
 147 respectively. Plot (e) and (f) compare with the MUSIC beamforming spectrum calculated with  
 148 the data in the red dashed box in (a) and (b), whose peaks indicate the wavefield direction of  
 149 propagation and its velocity. The channels used for MUSIC beamforming are from 12-77, indicated  
 150 by green dashed line in Figure 1a.



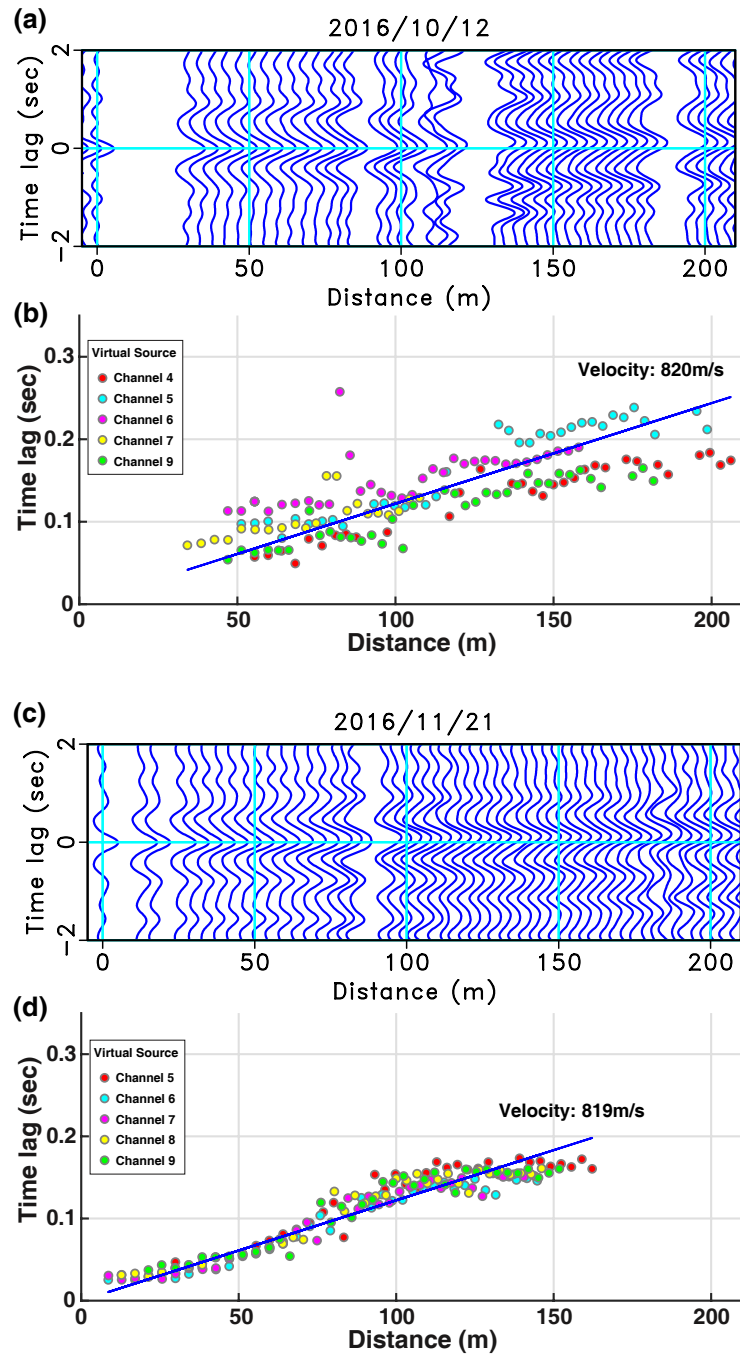
174 **4 Results**

175 Using data recorded at channels away from the construction site, we first estab-  
 176 lish the baseline velocity of the site and demonstrate that DAS recordings, after urban  
 177 noise removal, can provide reliable velocity estimates. We select the DAS array chan-  
 178 nels from 5-48, use 5 channels near channel 5 as virtual sources, and calculate the nor-  
 179 malized cross-correlograms. Figure 3a shows one of these normalized cross-correlograms  
 180 on 12 October 2016, whose vertical coordinate represents the seismic time lag from vir-  
 181 tual source to channels. The channels that are still contaminated by near-field noise af-  
 182 ter signal processing are omitted. Figure 3b shows the picked travel-time lag along the  
 183 distance, where the different colored dots denote the picks from different virtual sources.  
 184 Figures 3c and 3d are similar to Figures 3a and 3b but on 21 November 2016. The sur-  
 185 face seismic velocities are estimated by the least-squares slope of the scattered points on  
 186 each day. After correction for the propagation angle, the measured velocities on 10 dif-  
 187 ferent days show small variations over 3 months (Table S1 in supporting information).  
 188 The average velocity is measured at 816 m/s and the coefficient of variation is 3.2%, with  
 189 which the measurements at the construction site are benchmarked.

196 As acquisition moves closer to the construction site, effects of excavation on veloc-  
 197 ity are observed. We select two segments of the DAS recordings surrounding the con-  
 198 struction site, one on the south edge (Channels 170-184), and the other on the north edge  
 199 (Channels 108-128). Figure 4 shows the normalized cross-correlograms between Chan-  
 200 nel 36 (the green dot in Figure 1a) and the two segments before and after the excava-  
 201 tion. The measured arrival time shift in Figure 4 only depends on the velocity within  
 202 the footprint of the DAS array. In Figures 4a and 4b, we observe that before construc-  
 203 tion started the surface wave arrivals show high spatial coherency in both segments. Their  
 204 picked arrival times (red solid line) with slight moveout across the channels agree well  
 205 with the computed arrival times (pink dashed line) according to the average velocity of  
 206 816 m/s. Figures 4c and 4d show the cross-correlograms two weeks after excavation on  
 207 both segments. In Figure 4c, the south channels maintain the consistent arrival times  
 208 at the reference velocity, indicating a stable subsurface environment between the two in-  
 209 vestigations (as expected because no excavation was performed along this ray path). In  
 210 Figure 4d, systematic time delays are observed on the north segment, which suggests that  
 211 subsurface velocity between the two segments was reduced due to excavation of the base-  
 212 ment.

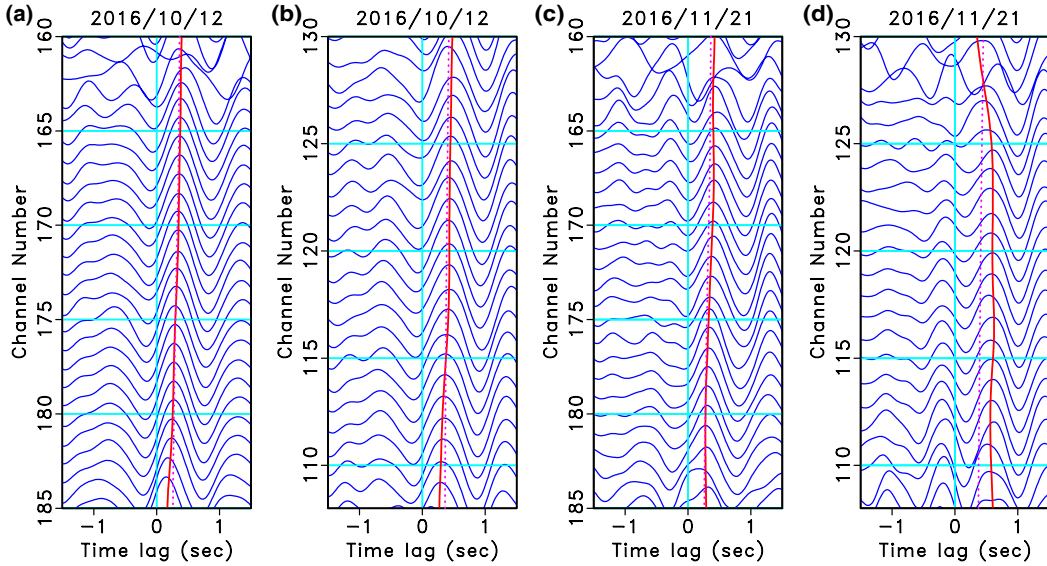
220 To investigate the spatial sensitivity of the passive DAS monitoring system, we ex-  
 221 tract surface wave velocities from Channels 162-205, where the construction site is be-  
 222 tween Channel 172 and 184. We use 3 channels near Channel 205 as virtual sources to  
 223 calculate normalized cross-correlations. Figure 5a and 5b show one of the cross-correlograms  
 224 (Channel 205 as virtual source) before and after the construction, respectively. The black  
 225 lines denote the picked travel time. Figure 5c plots the picked travel time versus distance  
 226 (green dots: before construction, red triangles: after construction). The picked travel times  
 227 stay within the same clusters with similar linear trends at channels east and west of the  
 228 basement. At the basement, however, the cluster of red triangles deviates from that of  
 229 the green circles, indicating significant changes in velocity.

230 The yellow dashed and blue solid lines are the least-squares piecewise linear fit of  
 231 the red triangles and green dots of the three parts. As expected, at both the west (chan-  
 232 nels 162-172) and east (channels 184-205) of the basement, the yellow and the blue lines  
 233 have very similar slopes. However, across the basement (channels 172-184) the yellow  
 234 line has a larger slope compared to the blue line, which indicates a smaller underground  
 235 velocity. Figure 5d plots the estimated average velocities along the three segments. Com-  
 236 paring the velocities before and after construction, it is obvious that the velocities to the  
 237 west and east of the basement are not significantly changed, whereas an obvious veloc-  
 238 ity drop from 824 m/s to 721 m/s is observed at the basement. The relative velocity drop  
 239 is 12.5%, nearly 4 times larger than the coefficient of variation 3.2% observed at stable



190 **Figure 3.** Five channels close to the channel 5 are used as virtual sources to calculate normal-  
 191 ized cross-correlograms with channels 5-48. Plot (a) shows the normalized cross-correlograms on  
 192 12 October 2016. Plot (b) shows the picked time lag along the actual spatial distances from all  
 193 the normalized cross-correlograms. The dots with different color denote the time delay picked  
 194 with different virtual sources. Plot (c) and (d) is similar to (a) and (b), but on 21 November  
 195 2016. The marked surface seismic velocities are calculated by the slopes of the blue lines.





213 **Figure 4.** Plot (a) and (b) compare the normalized cross-correlograms between the virtual  
 214 source (channel 36) and the front channels 165-183 and the back channels 108-136 on 12 October  
 215 2016, respectively. The virtual source is denoted by the green dot in Figure 1a. The front and  
 216 back channels are denoted by the orange and green lines in Figure 1a. Plot (c) and (d) are sim-  
 217 ilar to plots (a) and (b), but on 21 November 2016. The pink dashed lines show the calculated  
 218 time lag according to the reference velocity,  $816\text{ m/s}$ . The red solid lines show the picked time  
 219 lag of the normalized cross-correlation.

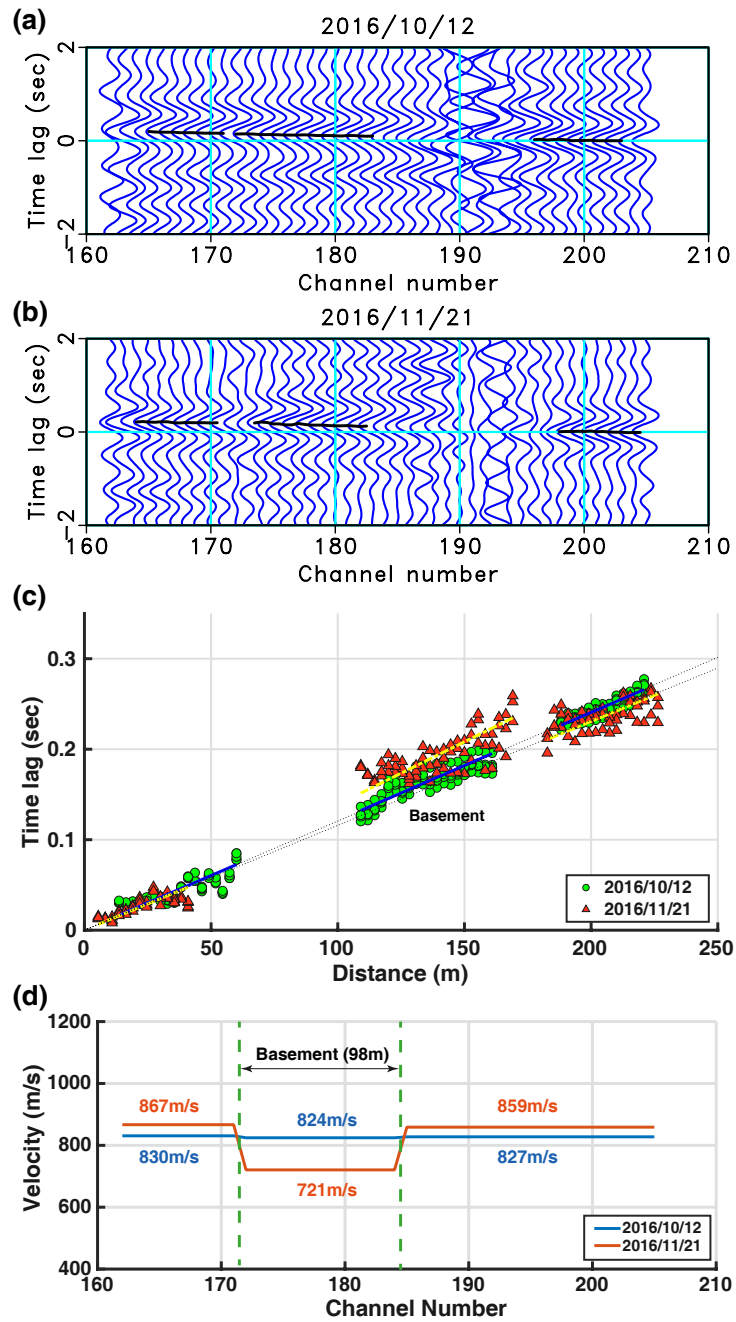
240 sections of the array. Therefore, we believe the velocity drop is statistically significant,  
 241 and caused by the excavation. This demonstrates the ability to detect changes due to  
 242 the excavation of a single building basement with unprecedented resolution for a DAS-  
 243 based urban seismic monitoring system.

## 251 5 Discussions

### 252 5.1 Observed velocity variations by DAS

253 Any monitoring system must strike an importance balance between its sensitivity  
 254 in detecting changes and its accuracy in issuing an alarm. In this study, we show that  
 255 the velocity measured using a DAS array does vary in time and space. Factors lead to  
 256 the velocity variations are three-fold: random DAS measurement error, changes in noise  
 257 fields, and changes in subsurface geological conditions. Through careful signal process-  
 258 ing, we have reduced the effect of DAS measurement noise, changes in noise fields and  
 259 source wavelet, so as to improve our ability to isolate changes due to subsurface geolog-  
 260 ical conditions.

261 Individual DAS channels have a lower signal-to-noise ratio (SNR) (Lindsey et al.,  
 262 2017; Yu, 2019) compared to conventional geophones in an ideal coupling condition. In  
 263 this experiment, the fiber cable is loosely lying in an existing conduit, which further re-  
 264 duces the SNR. Moreover, DAS recordings in urban areas are severely contaminated by  
 265 near-field noise. We observe a significant decrease in SNR after construction began. These  
 266 changes in the near-field noise, as well as any unknown changes in the surrounding noise  
 267 field, also cause variations in measured velocity. The combination of these two variations  
 268 are quantified using data recorded in a geologically stable zone, and later used as base-



244 **Figure 5.** (a) and (b): Normalized cross-correlograms on 12 October 2016 and 21 November 2016, respectively.  
 245 The black lines denote the picked travel time for three segments along the  
 246 fiber cable. (c) Picked time lags on 12 October 2016 (Green circles) and 21 November 2016 (red  
 247 triangles) plotted against distance. The gap from 60-100 meters distance are caused by removing  
 248 the poor quality data around channel 193. The yellow dashed lines and the blue solid lines are  
 249 least-squares linear fits to the red triangles and the green circles respectively. (d) Average veloci-  
 250 ties measured in three segments before and after excavation with a channel interval of 8.16m.

269 line statistics to identify abnormal velocity variations caused by changes in subsurface  
270 geology.

271 The measured velocity variation (12.5%) after excavation provides strong statisti-  
272 cal confidence of detection of an anomaly. On the other hand, the 3.2% baseline vari-  
273 ance suggests that small changes in subsurface velocity may not be identified by the DAS  
274 system, which may limit its applicability to identifying the development of small cavi-  
275 ties in urban environments.

## 276 5.2 Temporal resolution of DAS urban monitoring

277 Many of the passive seismic methods assume far-field and full azimuthal random  
278 sources with equipartitioning in energy (Roberts & Asten, 2008; Shapiro et al., 2005).  
279 However, urban ambient noise usually comes from fixed-location human activities that  
280 are often not perfectly random and isotropic (Bonnefoy-Claudet et al., 2006). When the  
281 sources are in close proximity to the array, longer recordings are used to increase the ran-  
282 domness and azimuthal coverage and reduce their susceptibility to near-field effects, par-  
283 ticularly for the low SNR DAS recordings.

284 In this experiment, we make use of the repetitive quarry blasts as far-field, unidi-  
285 rectional sources to extract subsurface velocity based on much shorter recordings than  
286 would be required for an ambient noise approach. The temporal resolution of our exper-  
287 iment depends on the interval of the blasts, a few days in this case, which is more rel-  
288 evant to urban subsurface monitoring and alert. When an array is placed closer to the  
289 quarry, abundant high-frequency signal should be recorded by DAS for higher resolu-  
290 tion subsurface monitoring.

## 291 6 Conclusions

292 Analysis of quarry blasts recorded by the Stanford Fiber Optic Seismic Observa-  
293 tory suggests that a surface DAS array in existing communication infrastructure can be  
294 used for time-lapse monitoring of near-surface velocity changes. Compared to a 3.2% base-  
295 line velocity variation, a strong velocity decrease (12.5%) is observed after two weeks of  
296 basement excavation. The high temporal resolution is achieved by making use of repet-  
297 itive quarry blast signals and a careful data processing workflow to remove the near-field  
298 noise and to normalize the variations in the blasting conditions. Our study suggests that  
299 a DAS array deployed in existing communication infrastructure has a strong potential  
300 for high-resolution urban near-surface monitoring and urban geohazard risk management.

## 301 Acknowledgments

302 We thank Biondo Biondi for inspiring us with this study and providing the DAS data.  
303 We are compiling the data for now. The two-day DAS data is include as supplements  
304 for review purposes. We acknowledge the EDB Petroleum Engineering Professorship and  
305 Cambridge Sensing Pte Ltd for financial support. Yunyue Elita Li is funded by MOE  
306 Tier-1 Grant R-302-000-182-114. Gang Fang is supported by National Natural Science  
307 Foundation of China (41504109). We also thank the Madagascar open-source software.

## 308 References

- 309 Ajo-Franklin, J. B., Dou, S., Lindsey, N. J., Monga, I., Tracy, C., Robertson, M., ...  
310 others (2019). Distributed acoustic sensing using dark fiber for near-surface  
311 characterization and broadband seismic event detection. *Scientific reports*,  
312 *9*(1), 1328.  
313 Biondi, B., Martin, E., Cole, S., Karrenbach, M., & Lindsey, N. (2017). Earthquakes  
314 analysis using data recorded by the stanford das array. *87th Annual Interna-*

- 315 *tional Meeting, SEG, Expanded Abstracts*, 2752-2756.
- 316 Bonnefoy-Claudet, S., Cotton, F., & Bard, P.-Y. (2006). The nature of noise wave-  
317 field and its applications for site effects studies: A literature review. *Earth-*  
318 *Science Reviews*, 79(3-4), 205–227.
- 319 Dahm, T., Heimann, S., & Bialowons, W. (2011). A seismological study of shallow  
320 weak micro-earthquakes in the urban area of hamburg city, germany, and its  
321 possible relation to salt dissolution. *Natural Hazards*, 58(3), 1111–1134.
- 322 Díaz, J., Ruiz, M., Sánchez-Pastor, P. S., & Romero, P. (2017). Urban seismology:  
323 On the origin of earth vibrations within a city. *Scientific reports*, 7(1), 15296.
- 324 Dou, S., Lindsey, N., Wagner, A. M., Daley, T. M., Freifeld, B., Robertson, M., ...  
325 Ajo-Franklin, J. B. (2017). Distributed acoustic sensing for seismic monitoring  
326 of the near surface: A traffic-noise interferometry case study. *Scientific reports*,  
327 7(1), 11620.
- 328 Douglas, I. (2004). People induced geophysical risks and urban sustainability. *Wash-*  
329 *ington DC American Geophysical Union Geophysical Monograph Series*, 150,  
330 387–397.
- 331 Gutiérrez, F., Parise, M., De Waele, J., & Jourde, H. (2014). A review on natural  
332 and human-induced geohazards and impacts in karst. *Earth-Science Reviews*,  
333 138, 61–88.
- 334 Jousset, P., Reinsch, T., Ryberg, T., Blanck, H., Clarke, A., Aghayev, R., ...  
335 Krawczyk, C. M. (2018). Dynamic strain determination using fibre-optic  
336 cables allows imaging of seismological and structural features. *Nature commu-*  
337 *nications*, 9(1), 2509.
- 338 Lindsey, N. J., Martin, E. R., Dreger, D. S., Freifeld, B., Cole, S., James, S. R., ...  
339 Ajo-Franklin, J. B. (2017). Fiber-optic network observations of earthquake  
340 wavefields. *Geophysical Research Letters*, 44(23), 11–792.
- 341 Martin, E. R., Huot, F., Ma, Y., Cieplicki, R., Cole, S., Karrenbach, M., & Biondi,  
342 B. L. (2018). A seismic shift in scalable acquisition demands new processing:  
343 Fiber-optic seismic signal retrieval in urban areas with unsupervised learning  
344 for coherent noise removal. *IEEE Signal Processing Magazine*, 35(2), 31–40.
- 345 Parker, T., Shatalin, S., & Farhadiroushan, M. (2014). Distributed acoustic sensing–  
346 a new tool for seismic applications. *first break*, 32(2), 61–69.
- 347 Renalier, F., Jongmans, D., Campillo, M., & Bard, P.-Y. (2010). Shear wave ve-  
348 locity imaging of the avignonet landslide (france) using ambient noise cross  
349 correlation. *Journal of Geophysical Research: Earth Surface*, 115(F3).
- 350 Roberts, J., & Asten, M. (2008). A study of near source effects in array-based (spac)  
351 microtremor surveys. *Geophysical Journal International*, 174(1), 159–177.
- 352 Schenato, L., Palmieri, L., Camporese, M., Bersan, S., Cola, S., Pasuto, A., ... Si-  
353 monini, P. (2017). Distributed optical fibre sensing for early detection of  
354 shallow landslides triggering. *Scientific reports*, 7(1), 14686.
- 355 Shapiro, N. M., Campillo, M., Stehly, L., & Ritzwoller, M. H. (2005). High-  
356 resolution surface-wave tomography from ambient seismic noise. *Science*,  
357 307(5715), 1615–1618.
- 358 Spica, Z., Pertou, M., Martin, E. R., Biondi, B., & Beroza, G. (2019, July 16). Ur-  
359 ban seismic site characterization by fiber-optic seismology. *EarthArXiv*.
- 360 Tran, K. T., & Sperry, J. (2018). Application of 2d full-waveform tomography on  
361 land-streamer data for assessment of roadway subsidence. *Geophysics*, 83(3),  
362 EN1–EN11.
- 363 Willis, M. E., Barfoot, D., Ellmauthaler, A., Wu, X., Barrios, O., Erdemir, C., ...  
364 Quinn, D. (2016). Quantitative quality of distributed acoustic sensing vertical  
365 seismic profile data. *The Leading Edge*, 35(7), 605–609.
- 366 Yu, Z. L. N. J. A. J. B., C. and Zhan. (2019). The potential of das in teleseismic  
367 studies: Insights from the goldstone experiment. *Geophys. Res. Lett.*, 46. doi:  
368 <https://doi.org/10.1029/2018GL081195>
- 369 Zhang, Y., Li, Y. E., Zhang, H., & Ku, T. (2019). Near-surface site investigation by



370  
371

seismic interferometry using urban traffic noise in singapore. *Geophysics*, 84(2),  
B169–B180.